

Property Transformation of Thermotropic Liquid Crystals Polymers

J. J. Rusek*

Purdue University, West Lafayette, Indiana 47907

and

K. P. Chaffee†

Air Force Research Laboratory, Edwards Air Force Base, California 93524

The advent of commercially available thermotropic liquid crystals polymers has led to novel uses of these plastics in the astronautics community. During the course of research, a fundamental property, termed polymers annealing, was empirically discovered, whereby thermal and chemical resistance of certain thermotropes are increased dramatically by a defined heat cycle after molding. A fundamental study of this annealing phenomenon has shown it to be a function of both rigid rod location and intermolecular forces. X-ray diffraction and atomic force microscopy results are shown to help in understanding the complex structure and surface morphology.

Introduction

POLYMERIC liquid crystal usage has been pervasive over the last three decades. Lyotropes are processed from acidic solution; the first commercial lyotrope, Kevlar®, has been used for body armor, heat shields, and structural components. The fundamental limitation of Kevlar's use is in its processing; the most convenient form processed is a drawn fiber. Although this geometry maximizes specific tensile strength, compressive properties of an ensemble of fibers are marginal. Macroscopic composites using lyotropic or graphite fibers dispersed in epoxy comprise the current state of the art.

Thermotropic liquid crystal polymers have been in existence for almost as long as the aforementioned lyotropes. These materials have not achieved the wide usage of the lyotropes because of high temperatures needed to process them and the relatively high cost compared to commodity resins. The conventional injection-molding philosophy is to include fillers such as talc or chopped glass fibers to impart isotropic behavior to the finished part. The inclusion of these fillers also reduces the final part's mechanical strength by averaging the oriented portions of the part with the off-axis portions.

A proposed way to design and produce a finished part is to injection mold the piece at minimum thickness, with no fillers. This assumes that only one preferred direction of strength is needed and that the high shear field of injection molding will create a thick enough boundary layer of highly oriented molecules. Because most real parts need strength in more than one direction at a time, this approach is flawed.

The rational approach to component design is to focus on the system and see how to manufacture a complete component, not a part to fit an existing geometry. This involves the use of alternative processing techniques, such as blow molding, extrusion, and compression molding in addition to injection-molding.

Before any design or bulk fabrication can be attempted, the dynamics of the molecular processes of the new material must be studied.

Chemistry

Polymeric liquid crystals are generally synthesized by a condensation polymerization. A typical lyotrope, poly (p-phenylene terephthalamide), is conveniently prepared by reacting p-phenylene diamine with terephthaloyl chloride in N-methyl-2-pyrrolidone. The repeat unit structure is shown in Fig. 1. An analogous thermotropic polymer, (1-phenylethyl-p-phenylene terephthalate), is produced by the reaction of 1-phenyl-ethyl hydroquinone with terephthaloyl chloride in methylene chloride using pyridine as an acid scavenger. The polymer repeat unit is shown in Fig. 2. A comparison of Figs. 1 and 2 shows the lyotrope to be a more compact molecule, hence the need for a solvent to cause flow. The thermotrope, on the other hand, is bulkier, lending itself to movement on the basis of thermal agitation alone. A side view of the molecules reveals a potential of the thermotrope to stack and lock via the pendant phenyl rings, causing a high degree of crystallinity. This molecular stacking manifests itself as a macroscopic annealing phenomenon that has been noted in certain liquid crystalline polymers. True physicochemical annealing obviates the melting point and improves solvent resistance by this effect of molecular stacking/locking.

This effect can be made clearer by first understanding that the ensemble of polymer molecules is observed to exhibit only a nematic phase. Figure 3 depicts the three phases of liquid crystalline behavior: nematic, smectic, and cholesteric. The thermotropic species under investigation in our research are all nematic, having orientation only in the direction of a general geometric director. This can be considered fortuitous in that this should not create any apparent fracture surfaces as would be expected in the smectic case. Unlike an isotropic metal, which contains small ($<0.4 \mu\text{m}$) atoms in a defined lattice, the polymer lattice is enormous, containing large ($5 \times 9 \mu\text{m}$) elliptical molecules. The intermolecular forces determine the ultimate mechanical properties of the polymer article; the rate of cooling then plays a profound part in this strength. Polymer annealing allows the molecules to have enough time to orient tightly with respect to each other.

Figure 4 shows the orientation of polymer fragments with respect to themselves. The model lyotrope shows a close packing, but it is quite evident that the model thermotrope forms a denser structure once locked. A polymer derived from this model has been synthesized and found to have no melt transition after procedural annealing.

The two largest practical problems to be overcome with the thermotropic species are determining heat-transfer rates and delineating the geometric boundaries of the annealing phenomenon. The definition of annealed regions is not straightforward; intense x-ray and neutron sources are required to define annealed regions precisely.

Received 30 December 1999; revision received 3 May 2002; accepted for publication 31 May 2002. Copyright © 2002 by the American Institute of Aeronautics and Astronautics, Inc. All rights reserved. Copies of this paper may be made for personal or internal use, on condition that the copier pay the \$10.00 per-copy fee to the Copyright Clearance Center, Inc., 222 Rosewood Drive, Danvers, MA 01923; include the code 0748-4658/02 \$10.00 in correspondence with the CCC.

*Adjunct Professor, School of Aeronautics and Astronautics, 1282 Grissom Hall. AIAA Member.

†Research Physicist, Propulsion Materials Applications Branch. AIAA Member.

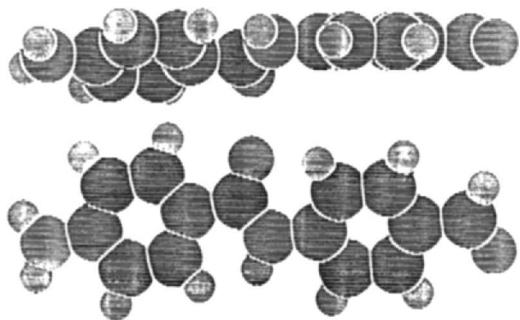


Fig. 1 Repeat unit of poly (p-phenylene terephthalamide) hydrogen connections added.

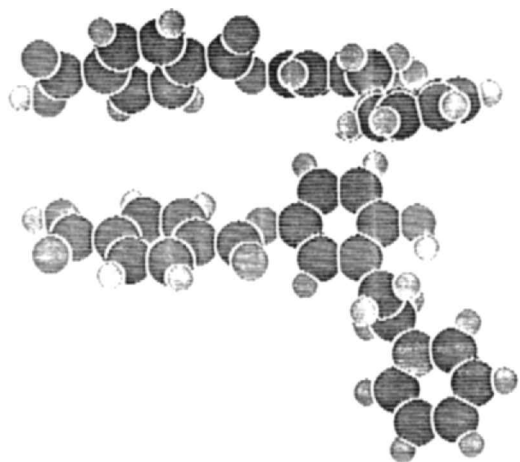


Fig. 2 Repeat unit of poly (l-phenylethyl-p-phenylene terephthalate) hydrogen connections added.

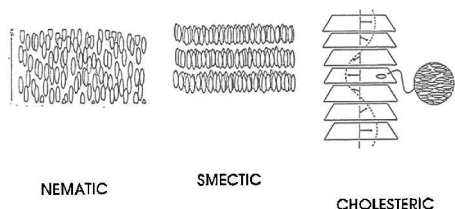


Fig. 3 Three phases of liquid crystalline behavior.

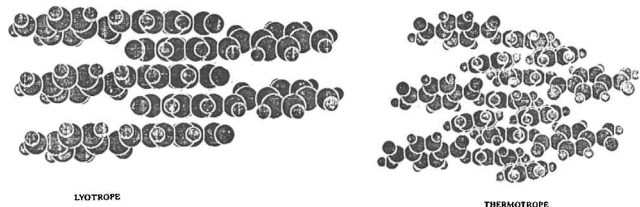


Fig. 4 Two-dimensional orientation of polymer fragments in model lyotropic and thermotropic cases.

This is currently done by sectioning molded parts and analyzing the end-capped group vs backbone atoms. The jump in this ratio defines an interfacial area where a high degree of orientation occurs.

X-Ray Diffraction

The XRD method applied in this study utilized x rays produced by a Philips Electronics XRG3100 generator operated at 45 kV and 30 mA. The diffraction patterns were created with nickel filtered copper K_α radiation ($\lambda = 1.54 \text{ \AA}$) and a flat plate camera with pin-hole collimation. Although accurate measurements of the diffracted x-ray location are easily obtained, the determination of quantitative intensity information from the photographic film is not possible.

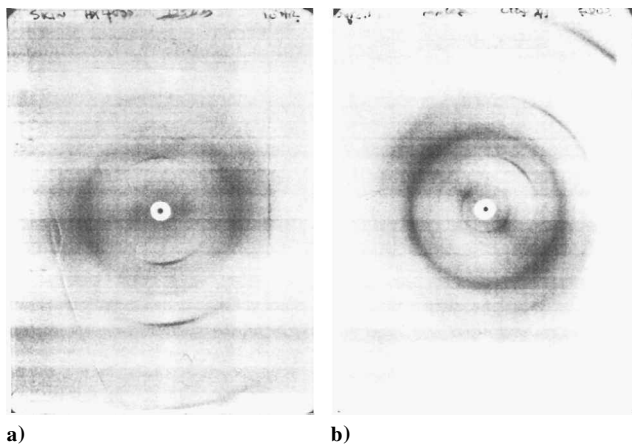


Fig. 5 X-ray diffraction patterns of Dupont HX-4000 polymer taken of a) skin and b) core regions.

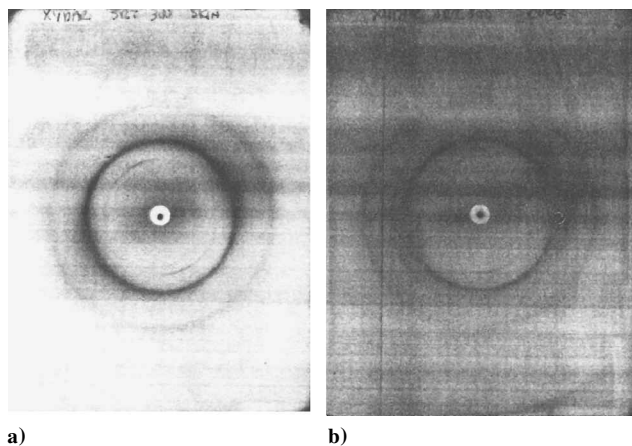


Fig. 6 X-ray diffraction patterns of Amoco XYDAR SRT-300 polymer taken of a) skin and b) core regions.

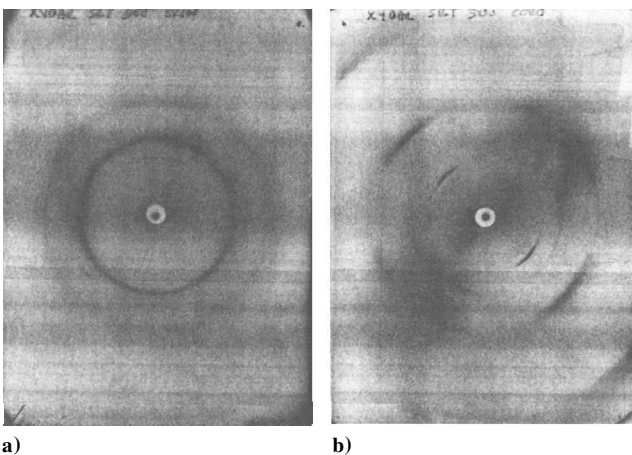


Fig. 7 X-ray diffraction patterns of Amoco XYDAR SRT-500 polymer taken of a) skin and b) core regions.

The "skin" and "core" samples were prepared by milling 175–300 μm thick plates from the appropriate regions of injection-molded thermotropic liquid crystalline polymer tensile specimens. The four commercially available polymers studied were XYDAR SRT-300 and SRT-500 (Amoco), HX-4000 (Dupont), and Vectra A950 (Celanese).

Figures 5, 6, 7, and 8 are the x-ray film exposures for HX-4000, SRT-300, SRT-500, and A950, respectively. The a and b portions of Figs. 5–8 denote skin and core regions, respectively. By measuring the ring radii and applying the Bragg relation, interatomic and

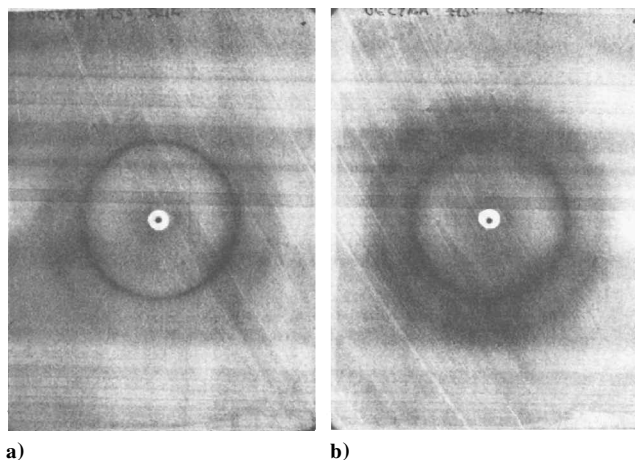


Fig. 8 X-ray diffraction patterns of Celanese VECTRA A950 polymer taken of a) skin and b) core regions.

intermolecular distances were calculated. The most striking observation is that all of the polymers, both in skin and core, exhibit an interatomic spacing 4.3 \AA . A calculated absolute minimum spacing based on the common pendant carbonyl group yields a value of 3.94 \AA , showing that the experimental value is an excellent agreement.

The patterns generated by both HX-4000 samples (Fig. 5) show no difference between the skin and core along the length of the molecule; however, a profound difference is noted between molecules. A common ring from 12.6 and 4.3 \AA is noted in both, but a double ring at 6.1 and 6.4 \AA is seen. These values do not fall in the range of harmonics and are indicative of a well-established crystalline domain in the core.

A comparison of Figs. 6a and 6b with Figs. 7a and 7b shows the polymers to have identical habits. There is no discernable difference along the polymer major axis in both SRT-300 and 500; however, there is a profound difference between each skin and core between polymer molecules. The core regions contain a much richer crystal habit (more developed) than the skin. This is noted by the more defined diffraction rings.

The Vectra A950 x-ray patterns, shown as Figs. 8a and 8b show more striking differences. The parallel axis distances are obviated within the core, whereas the skin shows a strong ring at 6.5 \AA . The intermolecular distances are the same for both skin and core. This is indicative of a total random mix of polymer rods in the core with locally established domains.

Atomic Force Microscopy

The atomic force microscope (AFM), introduced in 1986 by Gerd Binnig and Calvin F. Quate of Stanford University, is one of several scanning-probe microscopes that operates on similar principles as the scanning tunnel microscope (STM). The AFM allows three-dimensional imaging over a surface topography using a computer system that reproduces the images electronically on a color graphics monitor. The AFM consists of a shard of diamond fashioned into a sharp tip, which attaches to a metal cantilever about $100\text{--}200 \text{ }\mu\text{m}$ in length. The tip and a specimen are brought together close enough such that the electron clouds between the two repel. The specimen is then scanned under the tip in an X direction, while moving incrementally in the Y direction with each successive X scan. The STM senses surface morphology using a tunneling current rather than electrostatic repulsion and, therefore, is restricted to conductors and semiconductors. Deflections of the cantilever vary along the Z direction according to the surface relief. All three motions contribute to an image of the specimen's surface. Deflections of the cantilever result from electrostatic forces between the tip and the specimen, which can be an insulator, as well as a conductor. Deflections are detected by a laser beam from a laser diode focused on a spot on the back of the cantilever foil that reflects it to a photodiode sensor. Movements in all three directions are made pos-

sible by a rigid piezoelectric tubing on which the specimen rests. Piezoelectrics have the property of exhibiting mechanical strains, for example, expansion and contraction, when placed under an electric field. A feedback loop uses the deflected beam as an input to control Z movement created by the forces between the tip and specimen by applying a voltage to the Z portion of the piezoelectric tubing.

The data for the thermotropic liquid crystalline polymers presented here was acquired using a Digital Instruments NanoScope II. The images were obtained by the measurement of cantilever deflections as the polymers are scanned under the tip. The atomic forces involved are of the order of 10^{-9} N .

Four liquid crystal polymers were studied using the AFM, each having its surface characterized in two locations along the flow lines

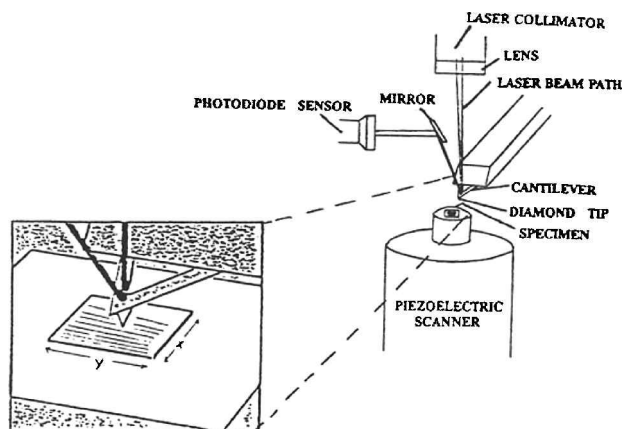


Fig. 9 Schematic of atomic force microscope.

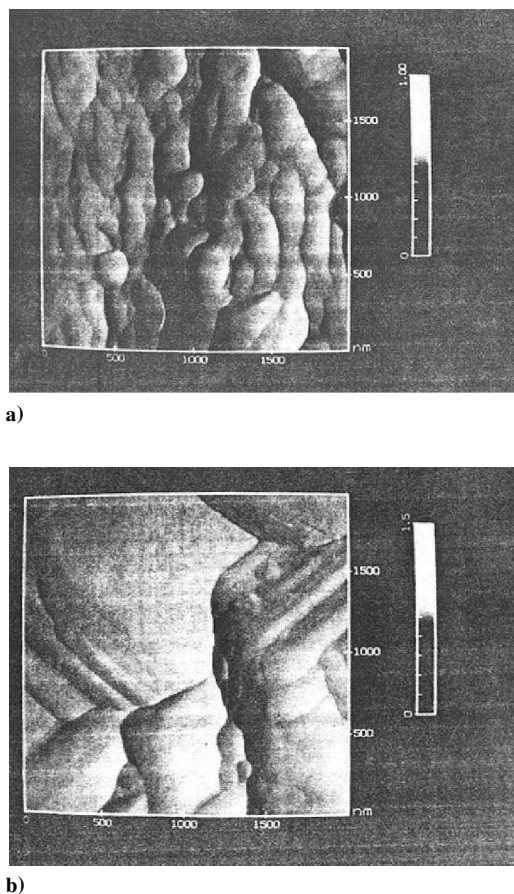


Fig. 10 AFM images of Dupont HX-4000 polymer taken of a) skin and b) core regions.

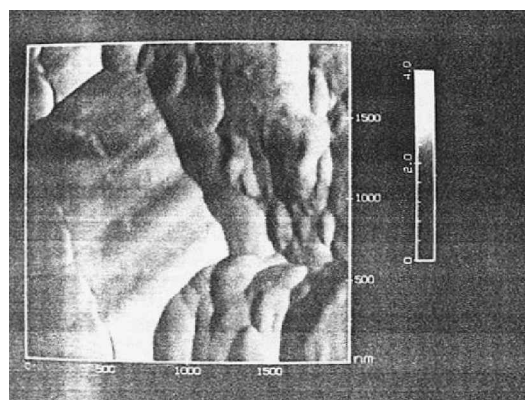
of the injection-molded material. One study was made immediately below the exterior portion of the skin, and the second study was within the interior or core region. Samples measuring 2 mm^2 were dissected from each region and supported on a magnetic disk that rests on the AFM scanner. These samples were held in place by double-sticktape and were made flat so that the AFM tip could track over its surface with little resistance. The cantilever tip scans each section perpendicular to the flow lines. Figure 9 shows a schematic of the AFM.

The AFM process under the best conditions proves to be time consuming and labor intensive. The microscopic roughness, characteristic of these samples, made scanning particularly difficult because the surface roughness often inhibited or broke the tip and cantilever. Images that are reproducible under many scans, at a scan rate of no more than 3.5 Hz, are illustrated in this report.

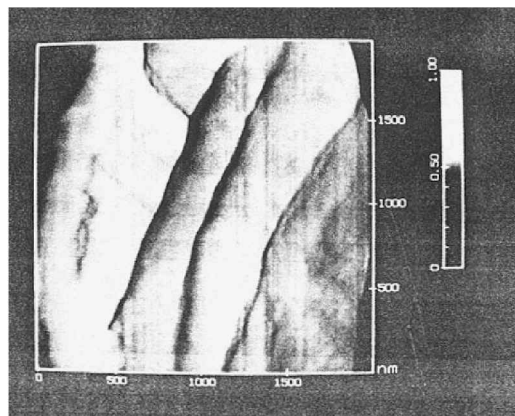
Figures 10, 11, 12, and 13 depict AFM images of HX-4000, SRT-300, SRT-500 and A950. Both skin and core samples are shown as parts a and b of Figs. 10–13, respectively. Scan size is 2000 nm in all cases. There is a pronounced difference between the skin and core sections; the skins show smaller crystallites, whereas the core sections show larger, well-defined crystalline regions. This observation is in agreement with the x-ray results discussed earlier.

The AFM images of HX-4000, shown as Figs. 10a and 10b both show the same orientation. The significant difference in skin and core is noted by the crystallite size. The skin shows average nodules that are 1×1 ellipses with widths of 300 nm, whereas the core shows 1×1 ellipses with average widths of 1000 nm.

Figures 11a and 11b show AFM images of SRT-300 in its skin and core regions. The skin region is highly oriented, with small crystallites, and the core shows large crystalline regions. Again, the skin crystallites are 1×1 ellipses, with an average 300-nm width.

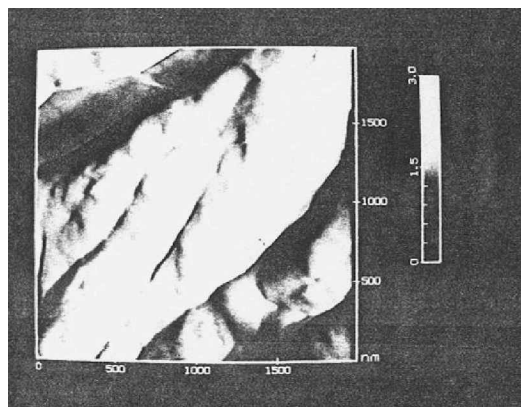


a)

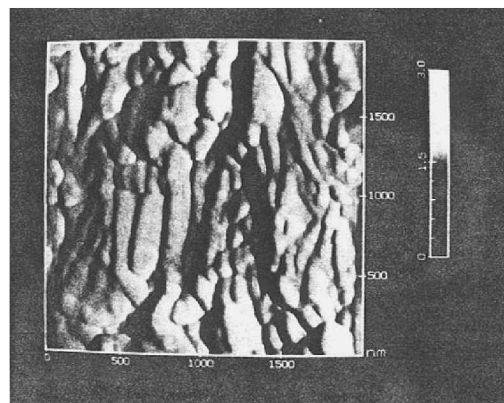


b)

Fig. 11 AFM images of Amoco XYDAR SRT-300 polymer taken of a) skin and b) core regions.

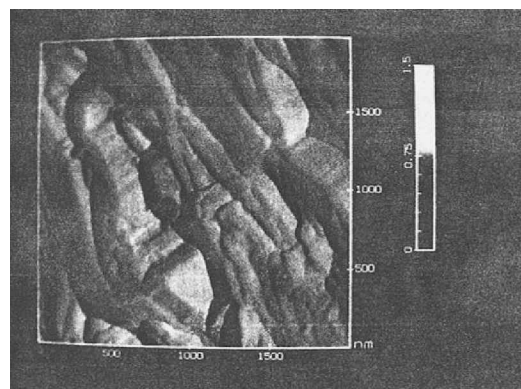


a)

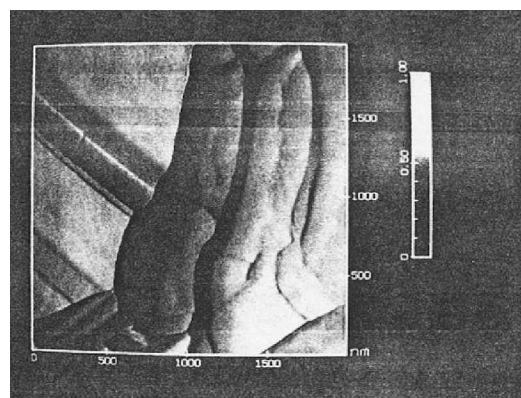


b)

Fig. 12 AFM images of Amoco XYDAR SRT-500 polymer taken of a) skin and b) core regions.



a)



b)

Fig. 13 AFM images of Celanese VECTRA A950 polymer taken of a) skin and b) core regions.

The significant difference is that the core contains 10×1 ellipses with 400-nm average widths.

The companion polymer, SRT-500, is shown by AFM images in Figs. 12a and 12b. This polymer has the most pronounced orientation difference between skin and core. The small crystallites in the skin exist as 200-nm 1×1 ellipses, whereas the core shows average crystallites of 400-nm width grown as 10×1 ellipses.

The final polymer, A950, is shown by its AFM images in Figs. 13a and 13b. The skin region is highly oriented along the flow axis, whereas the core is essentially isotropic, having a multitude of large crystalline regions at random orientations. The skin shows crystallites of 200-nm 1×1 ellipses, and the core shows average crystals of a 10×1 geometry having a width of 1000 nm.

Conclusions

It has been the intent of this paper to show the pronounced anisotropy that exists within injection-molded specimens of liquid crystal polymers. From this it is clear that the morphology and, hence, the physical properties, change within molded articles as a function of depth. This should be regarded as an excellent property of these materials because it is possible to produce rationally designed parts that behave as true molecular composites. The approach to arrive at this has been to use a diffraction technique and

a morphological technique in concert, resulting in the following conclusions:

- 1) Anisotropy exists between the so-called skin and core regions in the tested commercial liquid crystal polymer resins.
- 2) All of the analyzed polymers exhibited an interchain spacing of 4.3 Å.
- 3) The most isotropic core was shown to be Vectra A950.
- 4) All skins aligned with the formation of smaller nodules or crystallites.
- 5) All core formed large crystals. This phenomena was most probably due to the slow (>30 min) cooling of the part core.
- 6) HX-4000 was shown to have the same general crystal shape within the skin and core.
- 7) SRT-300 and 500 exhibited similar physical behavior, even though they are chemically different.

Acknowledgments

We would like to gratefully acknowledge Joseph Mallon and Patrick Adams of Aerospace Corporation for taking the x-ray data, David Silver of Edwards Air Force Base (AFB) for taking the Atomic Force Microscope data, and Christopher Frank of McClellan AFB and Rich Griffin of Hill AFB, who designed and manufactured the test specimen molds and dogbones.

TACTICAL MISSILE DESIGN

Eugene L. Fleeman, Georgia Institute of Technology

This is the first textbook offered for tactical missile design in 40 years. It is oriented toward the needs of aerospace engineering students, missile engineers, and missile program managers. It is intended to provide a basis for including tactical missile design as part of the aerospace engineering curriculum, providing new graduates with the knowledge they will need in their careers.

Presented in an integrated handbook method, it uses simple closed-form analytical expressions that are physics based to provide insight into the primary driving parameters for missile design. The text also provides example calculations of rocket-powered and ramjet-powered baseline missiles, typical values of missile parameters, examples of the characteristics of current operational missiles, discussion of the enabling subsystems and technologies of tactical missiles, and the current/projected state of the art of tactical missiles.

Included with the text is a CD-ROM containing electronic versions of the figures; 15 videos showing examples of loading missiles, pilot actions, flight trajectories, counter-measures, etc.; and configuration sizing methods.

AIAA Education Series

2001, 265 pp, Hardcover

ISBN 1-56347-494-8

List Price: \$94.95

AIAA Member Price: \$69.95

Source: 945



American Institute of Aeronautics and Astronautics

Publications Customer Service, 9 Jay Gould Ct., P.O. Box 753, Waldorf, MD 20604

Fax 301/843-0159 Phone 800/682-2422 E-mail aiaa@tascot1.com

8 am–5 pm Eastern Standard Time

Order 24 hours a day at www.aiaa.org

CA and VA residents add applicable sales tax. For shipping and handling add \$4.75 for 1–4 books (call for rates for higher quantities). All individual orders—including U.S., Canadian, and foreign—must be prepaid by personal or company check, traveler's check, international money order, or credit card (VISA, MasterCard, American Express, or Diners Club). All checks must be made payable to AIAA in U.S. dollars, drawn on a U.S. bank. Orders from libraries, corporations, government agencies, and university and college bookstores must be accompanied by an authorized purchase order. All other bookstore orders must be prepaid. Please allow 4 weeks for delivery. Prices are subject to change without notice. Returns in sellable condition will be accepted within 30 days. Sorry, we cannot accept returns of case studies, conference proceedings, sale items, or software (unless defective). Non-U.S. residents are responsible for payment of any taxes required by their government.

01-0346